

NOTE

Integrating a 1.5 T MRI scanner with a 6 MV accelerator: proof of concept

**B W Raaymakers¹, J J W Lagendijk¹, J Overweg², J G M Kok¹,
A J E Raaijmakers¹, E M Kerkhof¹, R W van der Put¹, I Meijising¹,
S P M Crijns¹, F Benedosso¹, M van Vulpen¹, C H W de Graaff¹,
J Allen³ and K J Brown³**

¹ Department of Radiotherapy, University Medical Center Utrecht, Heidelberglaan 100, 3584 CX, Utrecht, The Netherlands

² Philips Research Hamburg, Hamburg, Germany

³ Elekta, Crawley, UK

E-mail: B.W.Raaymakers@umcutrecht.nl

Received 2 April 2009, in final form 28 April 2009

Published 19 May 2009

Online at stacks.iop.org/PMB/54/N229

Abstract

At the UMC Utrecht, The Netherlands, we have constructed a prototype MRI accelerator. The prototype is a modified 6 MV Elekta (Crawley, UK) accelerator next to a modified 1.5 T Philips Achieva (Best, The Netherlands) MRI system. From the initial design onwards, modifications to both systems were aimed to yield simultaneous and unhampered operation of the MRI and the accelerator. Indeed, the simultaneous operation is shown by performing diagnostic quality 1.5 T MRI with the radiation beam on. No degradation of the performance of either system was found. The integrated 1.5 T MRI system and radiotherapy accelerator allow simultaneous irradiation and MR imaging. The full diagnostic imaging capacities of the MRI can be used; dedicated sequences for MRI-guided radiotherapy treatments will be developed. This proof of concept opens the door towards a clinical prototype to start testing MRI-guided radiation therapy (MRIgRT) in the clinic.

(Some figures in this article are in colour only in the electronic version)

1. Introduction

In modern radiotherapy, uncertainties about the location and shape of the tumour, and the surrounding organs at risk still pose a limitation on the maximum tumour dose. To guarantee tumour coverage during radiotherapy a margin around the tumour has to be treated as well. The unwanted result of this strategy is that also healthy tissue within this margin is treated and the maximum dose is determined by the toxicity to this healthy tissue.

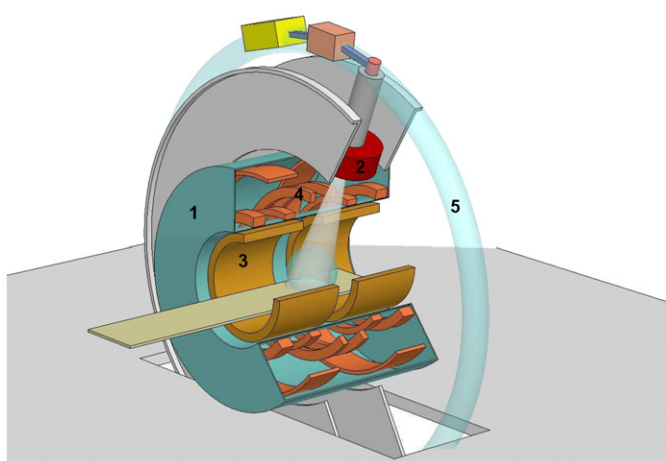


Figure 1. Sketch of the MRI accelerator concept. The 1.5 T MRI is shown in blue (1), the 6 MV accelerator (2) is located in a ring around the MRI. The split gradient coil (3) is shown in yellow and in orange the superconducting coils (4) are shown. The light blue ring around the MRI indicates the low magnetic field toroid (5) in the fringe field.

Image-guided radiation therapy (IGRT) aims to decrease the geometric uncertainties during radiotherapy by means of image guidance (Jaffray *et al* 2002, Smitsmans *et al* 2005, Berbeco *et al* 2004, Verellen *et al* 2007). In Lagendijk *et al* (2008) the use of MRI for radiotherapy guidance is presented: real-time MRI guidance allows better position verification but also the investigation of new treatment strategies for boosting the macroscopic tumour with stereotactic precision (Méndez Romero *et al* 2006, Lagerwaard *et al* 2008, Sonke *et al* 2008). This paper presents the proof of concept of integrating a 1.5 T MRI scanner and a 6 MV accelerator for real-time, MRI-guided radiotherapy.

2. System design

The concept of the MRI accelerator comprises a 6 MV Elekta (Crawley, UK) accelerator mounted on a ring around a modified 1.5 T Philips Achieva (Best, The Netherlands) MRI system. From the initial design onwards, modifications to both systems aimed to yield simultaneous and unhampered operation of the MRI and the accelerator. The radiation beam travels through the closed-bore MRI before it enters the patient. A sketch of the system concept is shown in figure 1.

For the prototype a static configuration is chosen to simplify the mechanical construction, as shown in figure 2. The accelerator is positioned laterally to the MRI system with a source–isocentre distance of 1.5 m. Given the 1 m radius of the MRI, the target is 0.5 m from the magnet surface. The accelerator, the MRI and the treatment room specifications and modifications will be discussed below.

2.1. Accelerator

The Elekta accelerator is a 6 MV standing waveguide with a dose rate of 350 cGy/min at 1 m. The collimation is done by means of cerrosafe blocks positioned in between the source and the magnet. The accelerator is modified by replacing various steel components by

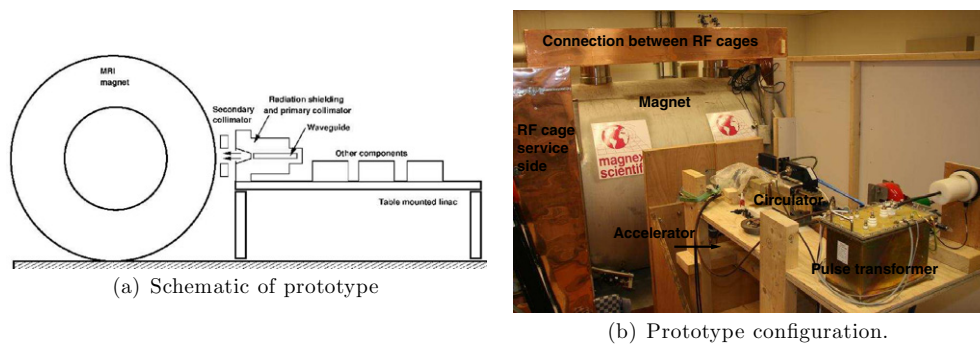


Figure 2. (a) A schematic overview of the configuration of the prototype (not to scale); a static position of the accelerator lateral to the MRI, with the source 0.5 m from the magnet surface, yielding a 1.5 m source–isocentre distance. (b) A photograph of the actual set-up. The accelerator is positioned on the wooden stand; the MRI is situated behind it. Also the copper RF cage at the service side of the MRI is visible.

non-ferromagnetic copies. It is mounted on a home-made wooden frame instead of on its steel gantry. The accelerator operates completely independent of the MRI system.

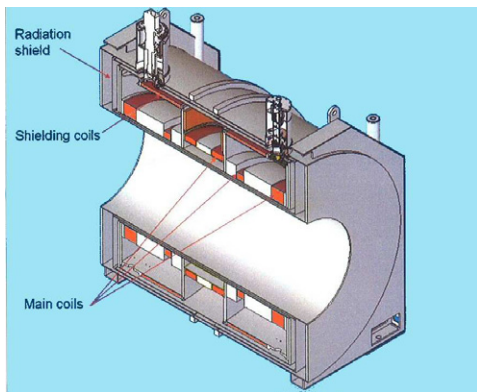
2.2. A 1.5 T MRI system

A modified 1.5 T Philips Achieva MRI system was used. As stated above, the MRI operates completely independent from the accelerator. A separate MRI console running the standard clinical Achieva control software is used to perform MRI. The entire library of Philips scan protocols is available. All standard 1.5 T Philips Achieva RF coils can be connected to the system; currently we have the Q body coil, the C1 surface coil and the head coil available. Since coils are interchangeable between Philips Achieva 1.5 T scanners, we also used a multi-channel (SENSE) body coil from one of our clinical systems.

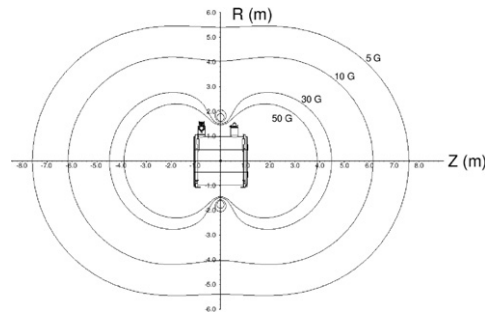
For this prototype, the magnet and the gradient coil are replaced by modified versions, as discussed below. The cryocooler, cooling cabinet, gradient- and RF-amplifiers as well as the reconstruction hardware are standard.

2.2.1. Magnet. The 1.5 T magnet was built by Magnex (Oxford, UK) and replaces the standard magnet in the Philips Achieva configuration. The central 15 cm are free of coils in order to let the radiation beam pass. This 15 cm gap allows a maximum irradiation field of 24 cm in the head–feet direction at the isocentre; see figure 3(a). Also the passive shimming system located inside the bore of the magnet is split in order to keep the central area free of shimming hardware. The total wall material is the equivalent of 8.2 cm of aluminium (including the gradient coil, see section 2.2.2). The central 15 cm is completely homogeneous. The two turrets are put aside to enable the placement of a ring gantry as shown in figure 3(a). The 1.5 T magnetic field has a homogeneity of 7 ppm over a 40 cm (radial axis) by 30 cm (longitudinal axis) ellipsoid.

The other adaptation is on the fringe field of the magnet. The magnet is actively shielded; most of the external field generated by the inner coils is cancelled by the field generated by a pair of shield coils with opposite polarity. This configuration is tuned such that a toroidal low-field zone is obtained (magnetic field lower than 10×10^{-4} T) with an inner radius of 1.6 m and an outer radius of 1.9 m, and a longitudinal width of 20 cm, located around the



(a) Cross section of the magnet (Courtesy of Magnex).



(b) Fringe field around the magnet.

Figure 3. (a) The cross section of the magnet. The superconducting coils are positioned outside of the central area and the two turrets are put aside to allow the construction of a ring gantry. (b) The mid-sagittal cross section of the fringe field with the low-field toroid around the magnet. The fringe field is rotational symmetric around the long axis of the magnet.

transverse midplane of the magnet; see figure 3(b). In this low-field toroid, the most sensitive parts of the accelerator are positioned. Now, in first order, the accelerator and the MRI are magnetically decoupled so that the MR images are not distorted by the presence of magnetized accelerator components, and the operation of the accelerator is not hampered by a too high external magnetic field.

Since the shape of the magnet differs from a standard Philips Achieva magnet, the standard covers do not fit. Therefore, we inserted home-made covers to ensure electrical safety and allow the MRI scanning of volunteers.

2.2.2. Gradient coil. The gradient coil was built by Futura (Heerhugowaard, The Netherlands) and replaces the standard gradient coil in the Philips Achieva configuration. The gradient coil was designed by Philips Research, Hamburg (Germany) and the central 19 cm are free from copper windings. The total radiation thickness of the gradient coil in the beam's eye view is 5 mm epoxy. The imaging performance is comparable with a standard Philips Achieva gradient coil.

2.3. Treatment room

The MRI accelerator is installed in a standard radiation treatment room with the beam facing the control room. Because of the fixed beam orientation a beam stopper is used to guarantee radiation safety in the control room. Furthermore, a quench pipe duct and two ducts for additional water cooling for the MRI peripherals are created in the roof of the treatment room.

Normally, an MRI is placed inside a Faraday cage to prevent external/ambient RF radiation from disturbing the MRI as well as to prevent the RF radiation used for MRI to disturb surrounding equipment. In our case, this would mean the accelerator and its peripherals should be placed inside this cage with potential RF interference between the MRI and the accelerator as a consequence. Therefore, the RF shielding of this experimental MRI was done

by placing two RF cages at both sides of the MRI bore. In this way, the inner wall of the MRI cryostat becomes an integral part of the RF cage, and the MRI sample volume is RF-wise shielded from the rest of the room including the accelerator.

Another issue is the magnetic fringe field outside the treatment room. In three adjacent rooms clinical Elekta accelerators are located. These are exposed to an additional magnetic field between 0.2 and 1.5×10^{-4} T (1 up to three times the earth's magnetic field). The standard control systems used for compensating the earth's magnetic field were used to successfully compensate for this additional magnetic field.

3. Performance tests of the MRI accelerator

The goal of this paper is to present the proof of concept of simultaneous MR imaging and irradiation. First the separate performance of the accelerator and the MRI will be presented, then the simultaneous irradiation and MRI will be shown.

3.1. Accelerator performance

Only a rudimentary test was performed on the accelerator output. A GafChromic film was positioned at the isocentre in the bore of the MRI and irradiated with a 5×5 cm² field. A dose of 4.2 Gy was delivered. This test merely showed that radiation can be delivered at the isocentre of this closed-bore MRI with the magnet on the field. Quantification of accelerator output, dose rate and scatter contamination is the topic of ongoing work.

3.2. MRI performance

Since the MRI is based on a Philips Achieva system we have the entire library of pre-defined diagnostic imaging sequences at our disposal. The initial tests consist of few standard imaging sequences for prostate, brain and kidney on volunteers, obviously with the accelerator switched off.

Prostate. In our clinic prostate delineation is done by combining MRI and CT (van Vulpen *et al* 2008). As an example of a T1 weighted spin echo (SE), a T2 weighted turbo spin echo (TSE) and a balanced steady-state-free precession (bSSFP) scan are presented. In figure 4, the scans as performed with the MRI accelerator in combination with a four-channel surface RF antenna (SENSE body coil, Philips, The Netherlands) are shown. The T1 SE, figure 4(a), has a repetition time (TR) of 663 ms and an echo time (TE) of 15 ms, a flip angle of 90° and an acquired voxel size of $1.00 \times 1.25 \times 3.00$ mm³. It clearly shows the prostate, rectum and bladder. The T2 TSE, figure 4(b), has a TR of 5989 ms and a TE of 120 ms, a flip angle of 90° and an acquired voxel size of $1.00 \times 1.50 \times 3.00$ mm³. The peripheral zone within the prostate can be distinguished on this scan. The bSSFP has a TR of 6.6 ms and a TE of 3.3 ms, a flip angle of 50° and an acquired voxel size of $1.77 \times 1.33 \times 2.03$ mm³. The latter yields an almost isotropic resolution in three dimensions and is therefore valuable for delineation of the prostate. While these scans are not optimized for this scanner, they yield diagnostic image quality.

Brain. The brain scans performed were a T1 weighted SE, a T2 weighted TSE and a 3D phase contrast angiogram. The scans in figure 5 were performed using the standard Philips Achieva head coil. In figure 5(a), the T1 weighted SE scan is shown with a TR of 596 and a

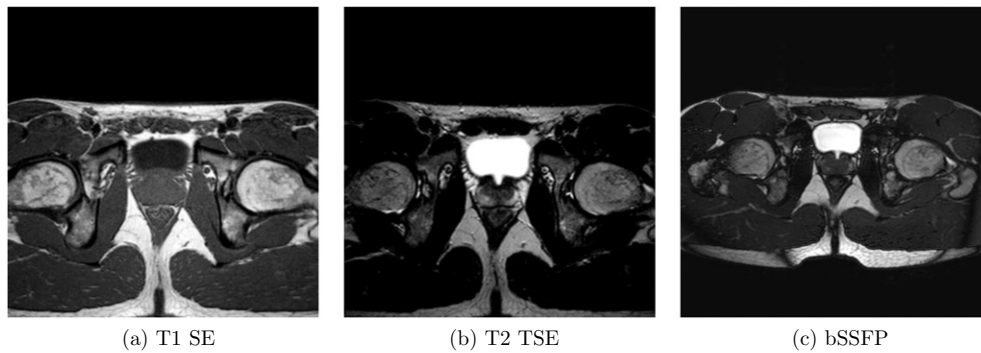


Figure 4. Prostate scans using a T1 SE sequence (a), a T2 TSE sequence (b) and a bSSFP sequence (c).

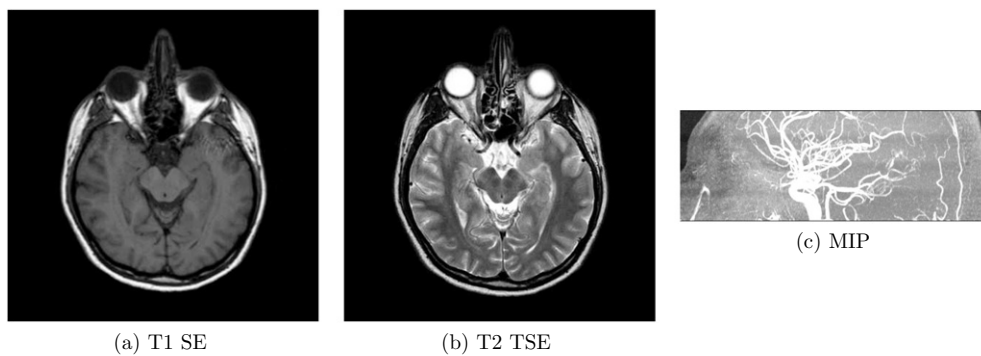


Figure 5. Brain scans using a T1 SE sequence (a), a T2 TSE sequence and the MIP of a phase contrast enhanced angiogram.

TE of 15 ms, flip angle 69° and an acquired voxel size of $1.02 \times 1.27 \times 5.00 \text{ mm}^3$. The T2 weighted TSE is shown in figure 5(b), TR 4892 ms, TE 110 ms, flip angle 90° and an acquired voxel size of $0.65 \times 0.84 \times 5.00 \text{ mm}^3$. In figure 5(c), the maximum intensity projection (MIP) of a 3D phase contrast enhanced sequence is shown, TR 25 ms, TE 6.9 ms, flip angle 20° and an acquired voxel size of $0.40 \times 0.70 \times 1.00 \text{ mm}^3$. This sequence exploits the artefact that results from blood flow and can be used to create an angiogram without intravenous contrast injection. Similar as for prostate, while these scans are not optimized for this scanner, they yield diagnostic image quality.

Kidney. The last example demonstrating the MRI performance is a dynamic sequence of 1 frame per second using a four-channel surface RF antenna (SENSE body coil, Philips, The Netherlands). It is a single slice T1 weighted ultrafast gradient echo, TR 592 ms, TE 100 ms, flip angle 90° and an acquired voxel size of $0.53 \times 0.54 \times 5.0 \text{ mm}^3$. Figure 6 shows two stills from the dynamic scan: the anatomy at the exhale state (figure 6(a)) and at the inhale state of the breathing cycle (figure 6(b)). Both kidneys, the liver and the spleen can be followed in time. At the caudal side, the sensitivity of the RF receive coil starts to decrease, resulting in a lower signal to noise ratio.

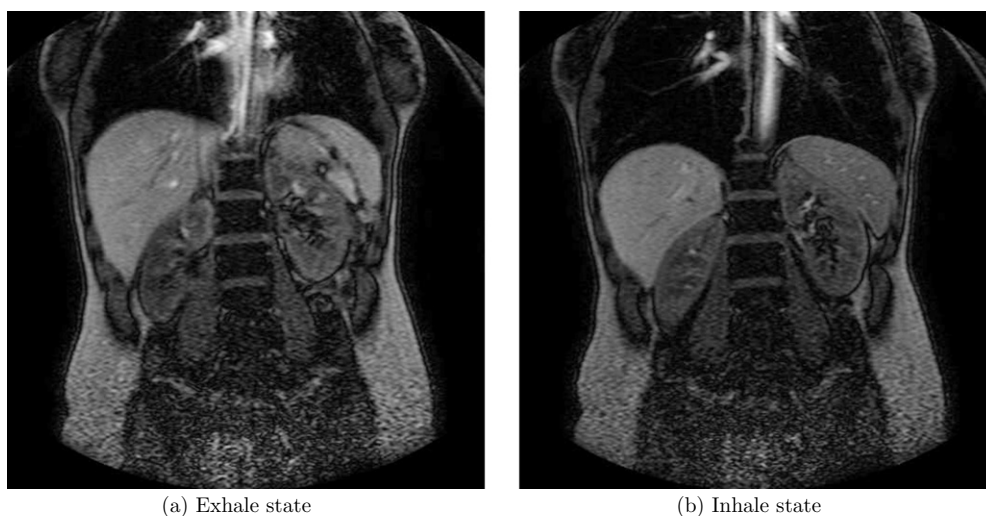


Figure 6. Stills from a dynamic scan of the kidneys, the anatomy in the exhale breathing state (a) and the inhale breathing state (b).

3.3. Simultaneous MRI and accelerator performance

The simultaneous operation of the MRI and accelerator has been tested on a piece of pork chop.

Pork chop. A piece of pork chop was simultaneously irradiated and imaged using a T2 weighted SE sequence using a C1 surface coil (Philips, Best, The Netherlands). The scan had a TR of 592 ms, TE 100 ms, flip angle 90° and acquired voxel size of $0.53 \times 0.54 \times 5.0 \text{ mm}^3$. The images with and without radiation beam on are identical, showing the proof of concept of simultaneous MR imaging and irradiation.

4. Discussion

The results show the possibility of simultaneous irradiation and 1.5 T MR imaging. The system was designed to obtain undistorted images with the radiation beam on as shown in figure 7.

The MRI offers diagnostic 1.5 T imaging quality, and we have the full library of Philips scan sequences at our disposal. Still, the optimal sequences for guiding radiotherapy treatments need to be determined. Diagnostic sequences are not necessarily the optimal sequences for treatment guidance. Together with Philips we will further investigate dedicated MR protocols in order to come to tumour-specific class solutions.

In the current work we used the standard Philips RF coils. These are not optimized with respect to radiation transparency, and when irradiated they will cast a shadow in the radiation field. Rieke *et al* (2005) showed already the feasibility of building x-ray compatible RF coils for their hybrid interventional MR/x-ray system (Fahrig *et al* 2001). Together with Philips, megavoltage (MV) transparent RF coils will be developed.

The prototype consists of a static accelerator MRI configuration. The next step towards a clinical prototype is including a multi-leaf collimator (MLC). This MLC will be located

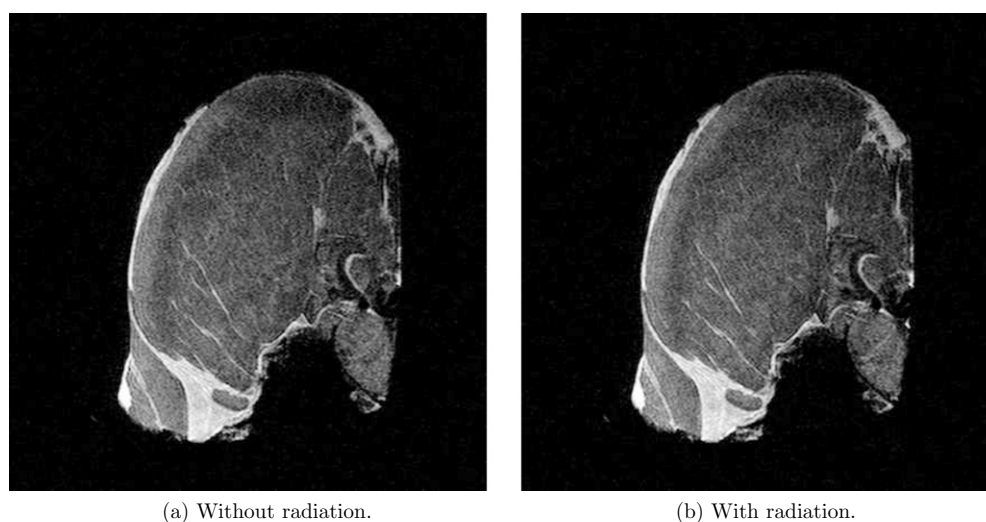


Figure 7. MRI of a pork chop with and without the radiation beam on.

outside of the low magnetic field region, and therefore together with Elekta a non-magnetic MLC will be constructed. Additionally, a gantry needs to be constructed in order to come to a fully rotating accelerator. This would then facilitate IMRT treatments, for instance, using an arc-therapy approach.

In order to introduce the MRI accelerator clinically, both the radiation dosimetry and the geometrical accuracy of the MR images need to be guaranteed (Moerland *et al* 1995). So far most work is done on the radiation dosimetry. Raaymakers *et al* (2004) showed that the dose distribution is affected by the presence of a magnetic field, especially at tissue–air interfaces (Raaijmakers *et al* 2005, 2007b). However, Raaijmakers *et al* (2007a) showed that using a multiple beam arrangement with a decent IMRT optimization yields exactly the same dose distribution with or without a magnetic field. Speeding up these calculation is the topic of current research. Recently, Meijsing *et al* (2009) showed that using an ionization chamber for dosimetry requires special attention regarding the orientation of the chamber with respect to the beam and the magnetic field. A detailed quantification of the accelerator radiation characteristics, including the impact of irradiating through the closed-bore MRI is being done.

5. Conclusion

The integrated 1.5 T MRI system and radiotherapy accelerator allow simultaneous irradiation and MR imaging. Both systems operate independently. The full diagnostic imaging capacities of the Philips MRI can be used; dedicated sequences for guiding radiotherapy treatments will be developed.

This proof of concept opens the door towards a clinical prototype to start testing MRI-guided radiation therapy (MRIgRT) in the clinic.

Acknowledgments

This research is supported by the Technology Foundation STW (applied science division of NWO and the technology programme of the Ministry of Economic Affairs) and by the Dutch

Cancer Society. Many thanks go to Jan van Ooyen and Arie van der Koppel from Philips Healthcare for installation of the MRI part of the system; their contribution enabled diagnostic imaging quality directly after installation.

References

- Berbeco R I, Jiang S B, Sharp G C, Chen G T Y, Mostafavi H and Shirato H 2004 Integrated radiotherapy imaging system (IRIS): design considerations of tumour tracking with linac gantry-mounted diagnostic x-ray systems with flat-panel detectors *Phys. Med. Biol.* **49** 243–55
- Fahrig R, Butts K, Rowlands J A, Saunders R, Stanton J, Stevens G M, Daniel B L, Wen Z, Ergun D L and Pelc N J 2001 A truly hybrid interventional MR/x-ray system: feasibility demonstration *J. Magn. Reson. Imaging* **13** 294–300
- Jaffray D A, Siewerdsen J H, Wong J W and Martinez A A 2002 Flat-panel cone-beam computed tomography for image-guided radiation therapy *Int. J. Radiat. Oncol. Biol. Phys.* **53** 1337–49
- Lagendijk J J W, Raaymakers B W, Raaijmakers A J E, Overweg J, Brown K J, Kerkhof E M, Van der Put R W, Hårdemark B, Van Vulpen M and Van der Heide U A 2008 MRI/linac integration *Radiother. Oncol.* **86** 25–9
- Lagerwaard F J, Haasbeek C J, Smit E F, Slotman B J and Senan S 2008 Outcomes of risk-adapted fractionated stereotactic radiotherapy for stage I non-small-cell lung cancer *Int. J. Radiat. Oncol. Biol. Phys.* **70** 685–92
- Meijsing I, Raaymakers B W, Raaijmakers A J E, Kok J G M, Hogeweg L, Liu B and Lagendijk J J W 2009 Dosimetry for the MRI accelerator: the impact of a magnetic field on the response of a Farmer NE2571 ionization chamber *Phys. Med. Biol.* **54** 2993–3002
- Méndez Romero A *et al* 2006 Stereotactic body radiation therapy for primary and metastatic liver tumors: a single institution phase i–ii study *Acta Oncol.* **66** 913–22
- Moerland M A, Beersma R, Bhagwandien R, Wijrdeman H K and Bakker C J G 1995 Analysis and correction of geometric distortions in 1.5 T magnetic resonance images for use in radiotherapy treatment planning *Phys. Med. Biol.* **40** 1651–64
- Raaijmakers A J E, Hårdemark B, Raaymakers B W, Raaijmakers C P J and Lagendijk J J W 2007a Dose optimization for the MRI-accelerator: IMRT in the presence of a magnetic field *Phys. Med. Biol.* **52** 7045–54
- Raaijmakers A J E, Raaymakers B W, van der Meer S and Lagendijk J J W 2007b Integrating a MRI scanner with a 6 MV radiotherapy accelerator: impact of the surface orientation on the entrance and exit dose due to the transverse magnetic field *Phys. Med. Biol.* **52** 929–39
- Raaijmakers A J E, Raaymakers B W and W Lagendijk J J 2005 Integrating a MRI scanner with a 6 MV radiotherapy accelerator: dose increase at tissue–air interfaces in a lateral magnetic field due to returning electrons *Phys. Med. Biol.* **50** 1363–76
- Raaymakers B W, Raaijmakers A J E, Kotte A N T J, Jette D and Lagendijk J J W 2004 Integrating a MRI scanner with a 6 MV radiotherapy accelerator: dose deposition in a transverse magnetic field *Phys. Med. Biol.* **49** 4109–18
- Rieke V, Ganguly A, Daniel B L, Scott G, Pauly J M, Fahrig R, Pelc N J and Butts K 2005 X-ray compatible radiofrequency coil for magnetic resonance imaging *Magn. Reson. Med.* **53** 1409–14
- Smitsmans M H P, De Bois J, Sonke J J, Betgen A, Zijp L J, Jaffray D A, Lebesque J V and Van Herk M 2005 Automatic prostate localization on cone-beam CT scans for high precision image-guided radiotherapy *Int. J. Radiat. Oncol. Biol. Phys.* **63** 975–84
- Sonke J J, Rossi M, Wolthaus J, van Herk M, Damen E and Belderbos J 2009 Frameless stereotactic body radiotherapy for lung cancer using four-dimensional cone beam CT guidance *Int. J. Radiat. Oncol. Biol. Phys.* **74** 567–74
- van Vulpen M, van der Heide U A and van Moerselaar J R 2008 How quality influences the clinical outcome of external beam radiotherapy for localized prostate cancer *Br. J. Urol.* **101** 944–7
- Verellen D, Ridder M D, Linthout N, Tournel K, Soete G and Storme G 2007 Innovations in image-guided radiotherapy *Nat. Rev. Cancer* **7** 949–60